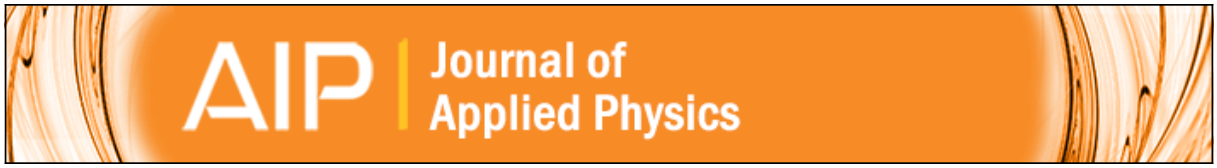

Influence of alternating current electrokinetic forces and torque on the elongation of immobilized DNA

W. A. Germishuizen, P. Tosch, A. P. J. Middelberg, C. Wälti, A. G. Davies, R. Wirtz, and M. Pepper

Citation: Journal of Applied Physics **97**, 014702 (2005); doi: 10.1063/1.1825627

View online: http://dx.doi.org/10.1063/1.1825627

View Table of Contents: http://scitation.aip.org/content/aip/journal/jap/97/1?ver=pdfcov

Published by the AIP Publishing

Influence of alternating current electrokinetic forces and torque on the elongation of immobilized DNA

W. A. Germishuizen, P. Tosch, and A. P. J. Middelberg
Department of Chemical Engineering, University of Cambridge, Cambridge, CB2 3RA United Kingdom

C. Wälti[a] and A. G. Davies
School of Electronic and Electrical Engineering, University of Leeds, Leeds, LS2 9JT United Kingdom

R. Wirtz and M. Pepper
Cavendish Laboratory, University of Cambridge, Cambridge, CB3 0HE United Kingdom

(Received 13 July 2004; accepted 30 September 2004; published online 16 December 2004)

The authors investigate the elongation and orientation of different-sized deoxyribose nucleic acid (DNA) molecules, tethered onto gold electrodes via a terminal thiol, under the influence of high frequency ac electric fields. The DNA molecules are elongated from a random coil into an extended conformation and orientated along the electric field lines as a result of the forces acting on the molecules during the application of the ac electric fields. Elongation was observed in the frequency range 100 kHz–1 MHz, with field strengths of 0.06–1.0 MV/m. Maximum elongation for all DNA fragments tested, irrespective of size, was found for frequencies between 200 and 300 kHz. The torque acting on the induced dipole in the DNA molecules, complemented by a directional bias force, opposite in direction to the dielectrophoretic force, provides the main contribution to the elongation process. The length of elongation is limited to either half the distance between opposing electrodes or to the contour length of the DNA, whichever is shorter. Further, the authors show that the normalized length of the elongated DNA molecules is independent of the contour length of the DNA. © *2005 American Institute of Physics*. [DOI: 10.1063/1.1825627]

I. INTRODUCTION

When a polarizable particle or molecule, such as deoxyribose nucleic acid (DNA), in an electrolyte is exposed to an ac electric field, a variety of forces act on the molecule. In the molecule itself, a dipole is induced as a result of the redistribution of charges at the molecule-electrolyte interface,[1] which, in a nonuniform field, leads to a dielectrophoretic force on the molecule. In addition, a torque, which aligns the dipole with the electric field,[1–4] is exerted on the molecule. This phenomenon is known as electro-orientation.[3] The applied ac electric field can also lead to fluid flow, which in turn can result in movement of the molecule.[3,5,6] The manipulation of small particles using dielectrophoresis and ac electrokinetic techniques in general has recently received considerable attention as an alternative to optical tweezers[7,8] or scanning probe techniques,[9,10] and is becoming a useful tool in molecular biology and biotechnology. Dielectrophoretic forces have been used to separate and manipulate cells,[2,11] bacteria,[12,13] viruses,[14] and submicron latex spheres.[5,15,16] Recently the dielectrophoretic manipulation of DNA molecules has led to applications such as the concentration of DNA molecules,[17–19] DNA-protein interaction studies,[20,21] and molecular surgery of DNA.[22]

However, a detailed understanding of the behavior of surface-immobilized DNA molecules when exposed to high frequency ac electric fields, and in particular the orientation and elongation of DNA as a result of dielectrophoretic force and torque, has not yet been established. This is partly owing to the complex local conditions that exist during application of the electric field. Orientation as a function of frequency, electric field, *p*H, and cation concentration has been studied using fluorescence anisotropy[23] and intensity measurements[17] to quantify the accumulation of DNA around the electrodes and the orientation of the DNA relative to the electric field lines. However, most DNA dielectrophoresis experiments reported in the literature were performed with fluorescently labeled DNA molecules free in solution which are attracted to the electrodes as a result of the imposed dielectrophoretic force. The increase in DNA concentration around the electrode edges leads to an increase in fluorescence intensity, which overshadows the fluorescence intensity changes as a result of dielectrophoretic orientation and elongation of the DNA. Direct immobilization of DNA onto the electrodes prior to electric field application removes this artifact and provides a direct means of studying the effects of the electric field on the molecule.[24]

In this article we present a detailed study of the effect of ac electric fields on the elongation and orientation of surface-tethered DNA molecules. We have immobilized four different-sized fragments of λ-DNA [15, 25, 35, and 48 kilobases (kb)] onto gold microelectrodes via a terminal thiol group, and measured the length of the elongated DNA as a function of electric field magnitude and frequency. We determine the optimum electric field and frequency range for effective manipulation of the DNA and investigate the elongation of the different-sized DNA fragments as a function of electrode separation. From these results a mechanism for orientation and elongation of immobilized DNA when exposed

[a]Author to whom correspondence should be addressed; electronic mail: c.walti@leeds.ac.uk

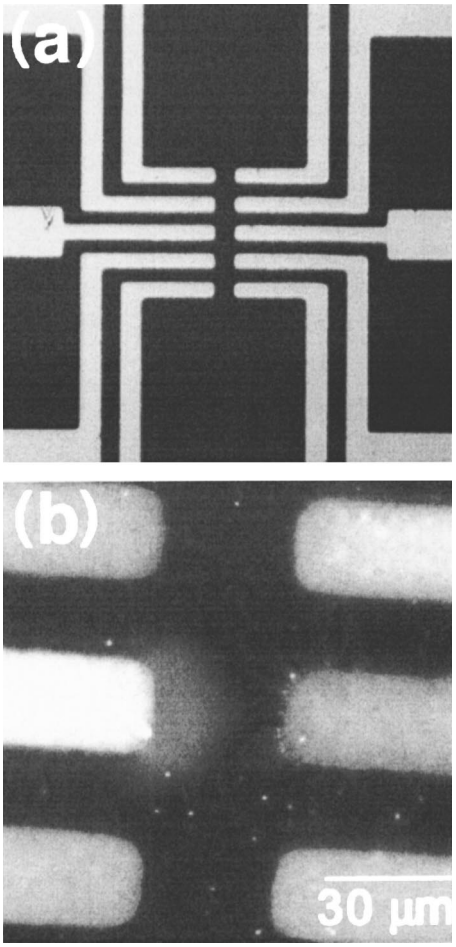

FIG. 1. (a) Bright-field photograph of the gold microelectrode array. (b) Fluorescent image showing an enlarged view of the electrodes. A 15 V, 300 kHz ac voltage was applied to the left middle electrode, resulting in the elongation of λ-DNA from the electrode edge. The DNA was fluorescently labeled with YOYO-1. The separation between opposite electrodes is 30 μm.

to an ac electric field is proposed, taking into account the theoretical electric field distribution and the observed fluid flow patterns near the electrodes.

II. MATERIALS AND METHODS

A. Microelectrode fabrication

Microelectrodes were used to generate the strong ac electric fields required for the DNA dielectrophoresis. An array of gold microelectrodes was evaporated onto a Si/SiO_2 substrate, using standard UV photolithography, metal evaporation, and lift-off. The 35-nm-thick gold electrodes were 30 μm in width and 15 μm apart. Gaps of 20, 30 μm, (Fig. 1) or 40 μm separated the opposite electrodes. Before DNA immobilization the wafer was cleaned by washing in "piranha" solution (30% H_2O_2, 70% H_2SO_4) for 1 h, followed by rinsing in de-ionized water, ethanol, and again in de-ionized water. All chemical reagents were purchased from Sigma-Aldrich, unless otherwise stated.

B. DNA fragment preparation

Full-length λ-DNA (48 kb) was used in the experiments, along with three smaller λ-DNA fragments (15, 25, 35 kb). λ-DNA is a double-stranded circular DNA molecule that contains two single-stranded nicks on opposite strands, 12 bases apart. The base pairs between the two nicks dissociate when heated to 65 °C, forming a linear molecule with two complementary single-stranded overhangs. The three DNA fragments were obtained by digesting λ-DNA with various restriction enzymes (New England Biolabs) as follows: the 15 kb fragment was formed by the digestion of λ-DNA with *Bst*Z17I; the 25 kb fragment by concurrent digestion with *Xba*I and *Nhe*I, and the 35 kb fragment by digestion with *Nhe*I. The solutions containing the restriction digests were heated to 65 °C to dissociate the 12-base overhang of the DNA before the digestion products were loaded onto a ethidium bromide-stained 0.5% agarose gel in tris-acetate-EDTA (TAE) buffer and separated by applying an electric field of 2 V/cm for 3 h. A well was cut in front of the fragments to be purified, and filled with 0.6% low melting point TAE agarose gel. Electrophoresis was continued until the DNA fragments of interest were within the low melting point gel. The gel piece containing the DNA fragments was excised, digested with Gelase (Epicentre), and purified by ethanol precipitation. Before immobilization of the DNA fragments onto the gold electrodes as described in detail in Ref. 24, each solution was diluted to 50 ng/μl DNA in TE (10 mM tris-HCl, 1 mM EDTA, *p*H 8) 1 M NaCl solution, and the YOYO-1 fluorescent intercalator (Molecular Probes, Eugene, OR, USA) was added at an intercalator to basepair ratio of 1:8. Control experiments to confirm that the DNA is tethered to the electrodes via one end only have been carried out. The detection method used to confirm the presence of the DNA targets the biotin attached to the free end.[25] All of the control experiments, either using no oligonucleotides at all, complementary but nonthiolated, or noncomplementary oligonucleotides in the multistep procedure,[24] demonstrated that no λ-DNA was bound to the surface in the absence of suitable anchor molecules confirming that the DNA is tethered only via one end. Further, tethered λ-DNA was digested with *Bgl*II which cleaves the DNA close to the biotinylated end. No biotin was detected in this case, confirming that the biotinylated end was not bound to the surface.

C. Dielectrophoresis experiments

The experiments were all carried out in de-ionized water as the suspending medium, with a conductivity of the order of 10^{-5} S/m. The electric field used for dielectrophoresis of the DNA was generated by applying an ac voltage across two opposing electrodes, i.e., an oscillating potential was applied to a specific electrode, while the electrode directly opposite was grounded. All other electrodes were left at a floating potential. The ac potential was generated by a 20 kHz–1.1 MHz signal generator and subsequently amplified using a custom-built amplifier. The electric field referred to in this work is the amplitude of the applied voltage divided by the distance between the electrodes.

The orientation and elongation of the fluorescently labeled DNA as a result of the dielectrophoretic force and torque exerted on the DNA was observed with a fluorescent microscope (BX60, Olympus) using a 50× objective. A cooled charge coupled device (CCD) camera (150CL, Pixera) was used to capture images of the elongated DNA. These images were analysed with Scion Image (http://www.scioncorp.com). Images were captured about 10 s after each parameter adjustment to allow steady-state conditions to be reached.

D. Analysis of fluid flow using latex beads

Fluorescently labeled latex beads (Sigma-Aldrich) were used to trace the fluid flow patterns during dielectrophoresis experiments. The latex beads, 0.5 and 2.0 μm in diameter, were carboxylate-modified and labeled with a red and yellow-green fluorescent dye, respectively. Before each experiment the beads were centrifuged at 15 000 × g for 10 min and washed in de-ionized water three times to remove the storage buffer and resuspended in de-ionized water to a concentration of 0.0125% solids. During application of the electric field the beads experience a combination of dielectrophoretic and hydrodynamic forces. However, their dielectrophoretic behavior is well studied[5,15,26,27] and was taken into account when interpreting their motion in the liquid.

E. Modeling of the electric field

In order to understand the effect of the electrode separation on the elongation and orientation of the DNA molecules, and thus to gain a more detailed understanding of the forces involved, we modeled the electric field around the electrode array using the finite element analysis software Femlab. Figure 2(a) shows the predicted electric field and the electric field lines between two electrodes, separated by a 30 μm gap. The center top electrode was set to a potential of 15 V, the center bottom electrode to 0 V, while all other electrodes were left floating. The electric field is highest directly at the electrode edges, as expected, and reaches a minimum halfway between the electrodes. The results shown in Fig. 2(a) are for calculations conducted in two dimensions and are only intended to give a qualitative indication of the field distribution. Figure 2(b) shows the magnitude of the electric field **E**, calculated in three dimensions, between the two center electrodes in the plane of the electrode surface. **E** is highest immediately adjacent to the electrode edges and decreases sharply to reach a minimum value at the center of the gap between the electrodes.

III. RESULTS AND DISCUSSION

In the experiments reported here, the DNA molecules were labeled with a fluorescent intercalator and thus their elongation resulted in the formation of an observable fluorescent band of DNA around the electrode edge [Fig. 1(b)]. Although previously dielectrophoretic force has been utilized to concentrate DNA free in solution at electrode edges,[17–19] in the experiments reported here, there was no free DNA in solution that could be attracted toward the electrodes; the fluorescent band around the electrode was solely due to the elongation of DNA molecules, attached to the electrodes by one end via a chemical bond that was formed before application of the electric field. The width of this fluorescent band is a direct measure of the extent of elongation of the immobilized DNA. In all experiments, the reported length of the DNA is the width of the fluorescent band measured from the electrode edge to the edge of the fluorescent band directly between the opposing electrodes. Experiments were repeated three times, and the results reported here are the average of the three experiments. Error bars, on average about ±0.5 μm, are omitted from the figures to improve presentation clarity.

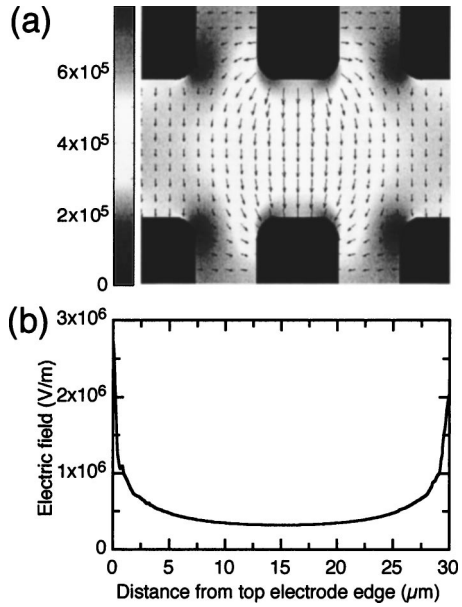

FIG. 2. (a) The electric field around the gold electrodes, calculated using Femlab software. The center top electrode was set to potential 15 V, the center bottom electrode to 0 V, and all other electrodes were left floating. The electric field was calculated in two dimensions. The arrows indicate the direction of the electric field lines. (b) The value of the electric field as a function of distance between the center top and bottom electrodes. The electric field was calculated in three dimensions, and the values shown here represent the electric field in the plane of the electrode surfaces.

A. Frequency and amplitude dependence of DNA elongation

Figure 3(a) shows the length of elongated DNA as a function of frequency at a voltage of 20 V applied across a 40 μm gap, resulting in an electric field of 0.5 MV/m. The behavior of all DNA fragments investigated was qualitatively similar. Below about 100 kHz and above 1.1 MHz the width of the fluorescent band was too small to be measured; we assume that the surface bound DNA molecules were not substantially elongated at these frequencies. A maximum elongation was observed around 200–300 kHz for all DNA fragments. Figure 3(b) shows the length of elongated 35 kb DNA fragments as a function of electric field at different frequencies, again for a 40 μm gap. The behavior is qualitatively similar at all frequencies, with elongations varying according to the findings in Fig. 3(a). Elongation of the DNA was only possible in fields higher than 0.06 MV/m, and increased with applied voltage up to about 20 V (0.5 MV/m), when

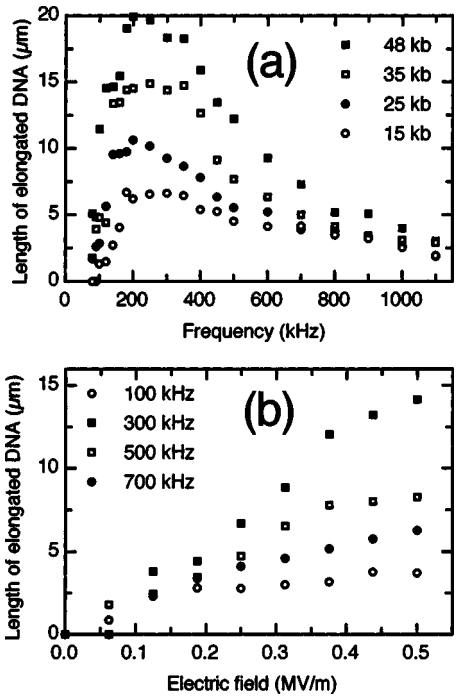

FIG. 3. (a) Length of elongated DNA as a function of frequency at an electric field of 0.5 MV/m across a 40 μm gap: 48 kb (*closed squares*), 35 kb (*open squares*), 25 kb (*closed circles*), and 15 kb (*open circles*). The DNA was immobilized onto the gold surface via a terminal thiol, using the multistep procedure and the length was measured from the electrode edge to the edge of the fluorescent band. (b) Length of elongated surface-bound 35 kb DNA across a 40 μm gap as a function of electric field at different frequencies: 100 kHz (*open circles*), 300 kHz (*closed squares*), 500 kHz (*open squares*), and 700 kHz (*closed circles*). Each value is the average of three experiments.

the increased electrothermal fluid flow prevented steady elongation of the DNA and thus formation of a stable fluorescent band, and length measurements were not possible. This will be discussed in more detail later. The other DNA fragments (48, 25, and 15 kb) showed similar results to the 35 kb DNA fragment (results not shown).

Unlabeled λ-DNA (48 kb) has a length of 16.5 μm when fully elongated,[28] but the intercalation of YOYO-1 at a dye: base pair ratio of 1:8 leads to a 20% increase in length.[29] Therefore, the contour length L_0 of the 48 kb DNA is about 20 μm. The contour lengths of the shorter fragments were calculated in the same way yielding a contour length L_0 of about 15 μm for the 35 kb DNA, of about 11 μm for the 25 kb DNA, and of about 6.5 μm for the 15 kb DNA. Figure 3(a) shows that all four DNA fragments were fully elongated at around 250 kHz.

Several forces act on the immobilized DNA molecules during dielectrophoresis, and these will now be discussed in order to establish a possible elongation mechanism. In a spatially nonuniform electric field **E**, different forces act on different parts of the DNA molecule as the electric field interacts with the induced dipole along the backbone of the molecule. The net time-averaged dielectrophoretic force, $\mathbf{F}_{\mathrm{DEP}}$, results in a movement of the DNA in the direction of the highest values of the product $\mathbf{E}\cdot\nabla\mathbf{E}$, i.e., toward the electrode edges, and is given by $\mathbf{F}_{\mathrm{DEP}}=1/4\,\alpha v\nabla|\mathbf{E}|^2$, where α is the polarizability and v the volume of the particle.[1,4] In addition, a torque $\mathbf{T}=\mathbf{p}\times\mathbf{E}$ is exerted on the induced dipole by the electric field, where $\mathbf{p}=\alpha v\mathbf{E}$ is the induced dipole. In contrast to the dielectric force, the torque depends on the electric field but not its gradient, and thus can be finite even in a uniform field. The torque causes an alignment of the induced dipole along the electric field lines.[3]

The behavior of charged polymeric molecules such as DNA when pulled by external forces, for example in an electric field, can be described by the wormlike chain (WLC) model.[30] The WLC model is a special limit of the Kratky–Porod (KP) model,[31] where the molecule is approximated as a succession of N segments of length b. The WLC approximation is the continuous limit of the KP model, i.e., $b\to 0$. A possible mechanism for the elongation of the DNA in an ac electric field has been discussed in Ref. 32. The individual segments align with the electric field lines owing to the torque **T** and there are two energetically favorable orientations for each segment, parallel and antiparallel to the field lines. In a strong electric field ($E\gg\sqrt{k_bT/\alpha}$, where T denotes temperature, k_b is the Boltzmann constant, and E is the absolute value of **E**), but with no additional external force pulling on the DNA, the segments align with equal probability parallel or antiparallel with the field and the mean elongation of the DNA molecules is expected to be small.[32] However, in the presence of an external or bias force pulling outwards from the electrodes, the probability distribution is shifted toward parallel alignment and an elongation of the DNA molecule results. It has been shown theoretically that a reduction of the torque leads to a decrease in elongation for the same bias force.[32]

We note that the dielectrophoretic force points toward the electrodes and is therefore unlikely to contribute towards elongation of the immobilized DNA molecules. Thus other forces, such as viscous drag resulting from fluid flow, have to be considered. In the presence of an electric field, forces act on charges and dipoles in the fluid, leading to fluid flow. In the frequency and electric field range covered in this work, two types of fluid flows are present and have to be taken into account. At low frequencies, i.e., below about 100 kHz dependent on the electrode geometry, the dominant fluid flow is ac electro-osmosis.[5,6] ac electro-osmosis decreases with increasing frequency and at high frequencies, i.e., above 500 kHz–1 MHz, the dominant force is electrothermally induced fluid flow.[6,33]

We have investigated the fluid flow as a function of frequency and electric field in the same system used for studying the elongation of DNA. Figure 4(a) shows a frame of a video recording of the motion of the latex beads during the application of a 1 MHz, 0.25 MV/m electric field. The arrows indicate the fluid flow pattern, which was derived from the migration of the latex beads while taking into account the dielectrophoretic effect of the electric field on them. The 0.5 μm beads experience positive dielectrophoresis in deionized water (conductivity of the order of 10^{-5} S/m), while the 2.0 μm beads experience negative dielectrophoresis over the frequency range investigated.[15,26] At lower electric field magnitudes, the 0.5 μm red fluorescent beads were attracted to the electrode edges, as expected from positive dielectrophoresis, while the 2.0 μm green fluorescent beads remained

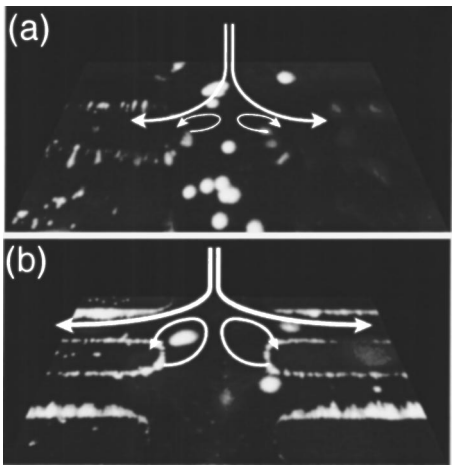

FIG. 4. Frames of a video recording of 0.5 and 2.0 μm fluorescently labeled latex beads during application of a (a) 1 MHz and a (b) 100 kHz ac electric field with a magnitude of 0.25 MV/m. The arrows indicate the direction of the fluid flow in each case, derived from studying the movement of the latex beads as a function of electric field magnitude and frequency. The line thickness of the arrows indicates the relative fluid velocities observed.

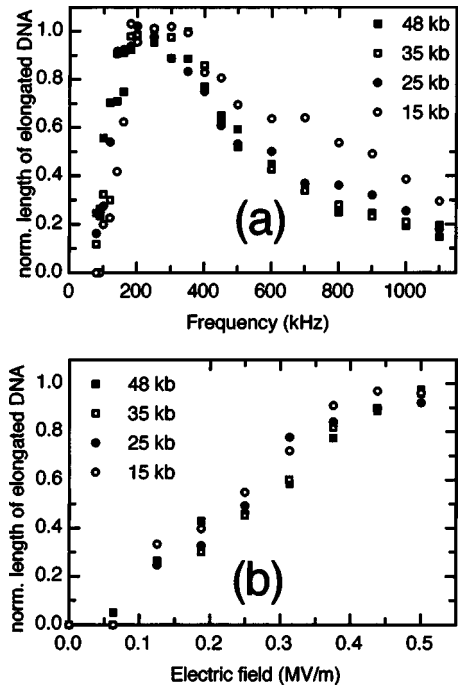

FIG. 5. (a) Normalized length of elongated DNA as a function of frequency at an electric field of 0.5 MV/m across a 40 μm gap: 15 kb (*open circles*), 25 kb (*closed circles*), 35 kb (*open squares*), and 48 kb (*closed squares*). The measured DNA length was divided by the theoretical length of the DNA fragment. (b) Normalized length of elongated surface-bound DNA across a 40 μm gap as a function of electric field at 300 kHz: 15 kb (*open circles*), 25 kb (*closed circles*), 35 kb (*open squares*), and 48 kb (*closed squares*).

stationary. As the electric field magnitude increased, the 0.5 μm beads started to migrate outward from the electrode edges despite their dielectrophoretic attraction to the electrodes, and the 2.0 μm beads began migrating downwards from the area above the electrodes toward the plane of the electrodes, where they were repelled from the electrodes and collected in the area between the electrodes.

The fluid flow at 100 kHz [Fig. 4(b)] exhibited a qualitatively similar pattern to that at 1 MHz, but the velocity of the fluid at corresponding electric field magnitudes was substantially higher at the lower frequency. As above, the 0.5 μm beads were attracted to the electrode edges at low electric fields, while the 2.0 μm beads experienced only limited movement. However, as the electric field increased to 0.25 MV/m, the 0.5 μm beads were repelled from the electrode edges towards the center of the gap between the two electrodes. The 2.0 μm beads migrated towards the gap between the electrodes, where they were pushed away at a high velocity just above the plane of the electrodes by the strong fluid flow [Fig. 4(b)]. The fluid flow at the lowest investigated frequency (45 kHz) was qualitatively the same as at 100 kHz but was quantitatively stronger. At all the frequencies investigated in this work, the direction of the fluid flow in the plane of the electrodes is from the electrode edges towards the center of the gap between them.

It has been shown previously that fluid flow can lead to the elongation of immobilized DNA molecules.[34,35] However, elongation of the DNA in this study cannot be attributed to fluid flow alone. The decrease of the elongation of the DNA with increasing frequencies above 300 kHz followed the same pattern as the decrease in fluid flow, suggesting some influence of the fluid flow on the elongation of DNA, while the opposite was found at low frequencies. No measurable elongation was observed for frequencies below about 100 kHz, whereas the fluid flow at 45 kHz was substantially higher than at 300 kHz, where the elongation of the DNA was maximal. At frequencies below 100 kHz, the effective electric field is reduced owing to electrode polarization[6,36] leading to a substantial decrease in the dipole moment and thus the dielectrophoretic torque. This suggests that a combination of the torque and the viscous drag force exerted on the DNA molecules result in the elongation of the DNA over the frequency range investigated. The fluid flow most likely provides the required directional bias to the torque resulting in elongation of the DNA molecules. Even though the fluid flow and thus the bias force increase with decreasing frequency, the reduced torque is not sufficient to overcome thermal randomization.

The decrease in length of the elongated DNA as a function of frequency above about 300 kHz [Fig. 3(a)] results from a combination of the decrease of the force pulling the DNA molecules away from the electrodes and a reduction of the dielectrophoretic torque. The reorientation of the charges along the backbone of the DNA starts lagging behind the switch in the polarity of the electrodes in the ac field with increasing frequencies, leading to a decrease of the effective dipole moment and thus torque.[3,24]

Figure 5(a) shows the normalized length $L_n = L/L_0$, where L is the measured length and L_0 the contour length, of the four elongated DNA fragments as a function of frequency at an electric field of 0.5 MV/m across a 40 μm gap. As also shown before, all the different fragments were fully elongated at frequencies of 200–300 kHz. Figure 5(b) shows L_n of the same fragments as a function of applied electric field. The data were taken in an electric field of 300 kHz across a 40 μm gap. In the previous paragraph we showed that the length of the elongated DNA fragments increases with increasing contour length. In contrast, the normalized length L_n

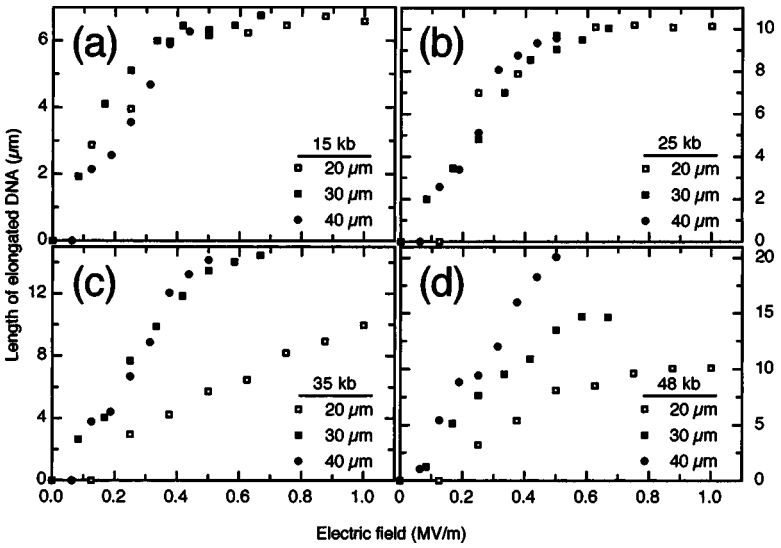

FIG. 6. (a) The length of elongated and immobilized 15 kb DNA as a function of electric field at different electrode separations: 20 μm (*open squares*), 30 μm (*closed squares*), and 40 μm (*closed circles*). (b) shows the results for 25 kb DNA, (c) for 35 kb DNA, and (d) for 48 kb DNA, respectively. A maximum voltage of 20 V was applied across the electrode gap, and electric field frequency was 300 kHz in all the cases.

only depends on the amplitude and frequency of the electric field, not on the contour length of the DNA. We note that the 15 kb fragments show deviations from the general behavior at high frequencies, probably owing to errors in the length measurements becoming large relative to the contour length of the DNA.

The results shown in Fig. 5 suggest that the mean elongation per unit length neither depends on the contour length of the DNA nor on the position of the segment of interest, i.e., on the distance from the electrode. In solution, the DNA molecule is surrounded by positive counter ions. The large contour lengths of the DNA fragments make it unlikely that the counter ions migrate all the way along the length of the DNA, and the counter ions are spatially restricted to short segments of the DNA.[37,38] Because the counter ions are uniformly distributed the torque acting on each segment is uniform. Therefore, we conclude that the total force acting on each segment is uniform over the majority of the molecule, again suggesting that the dielectrophoretic force plays only a minor role in the elongation of the immobilized DNA.

B. Influence of electrode separation

The forces responsible for elongating the surface-bound DNA depend on the electric field distribution across the gap between the electrodes. It may be expected that reducing both the gap size and the applied potential by an equivalent factor would not change the dielectrophoretic behavior of the DNA as the electric field does not change significantly. However, in the experiment we do observe changes in the behavior of the DNA, indicating that processes other than dielectrophoresis are important. Figures 6(a)–6(d) show the elongation of 15 kb (6.5 μm), 25 kb (11 μm), 35 kb (15 μm), and 48 kb (20 μm) DNA, respectively, as a function of electric field at various electrode separations. The frequency of the electric field was 300 kHz in all cases. In Figs. 6(a) and 6(b) [15 kb (6.5 μm) and 25 kb (11 μm)] the elongation of the DNA did not depend on the electrode separation and the behavior was very similar in all three cases. The DNA was elongated to its full contour length at sufficiently strong electric fields, irrespective of the electrode separation. Figure 6(c) shows the same measurements for the 35 kb (15 μm) DNA, but only the experiments with electrode separations of 30 and 40 μm showed similar behavior to the 15 kb (6.5 μm) and the 25 kb (11 μm) DNA fragments, i.e., full elongation at sufficiently strong fields, whereas the experiments performed on the 20 μm gaps only led to substantially reduced elongation. This effect is even more pronounced in the case of the 48 kb (20 μm) DNA, where only the experiments on the 40 μm gap led to the full elongation of the DNA molecules. Figures 6(c) and 6(d) suggest that the DNA molecules can only be elongated to half the distance between the electrodes if the gap is smaller than twice the length of the molecules, irrespective of the applied electric field. We note that for all the different-sized DNA fragments stable elongation was not possible when voltages of more than 20 V were applied, irrespective of the electrode gap size.

These findings are compatible with the elongation mechanism discussed earlier, where the bias force required to elongate the DNA molecules, in this case the fluid flow, changes direction halfway between the electrodes. An increase of the field only leads to a stronger bias force and not to further elongation of the molecule. This phenomenon is shown in Figs. 6(c) and 6(d), where the 35 kb DNA (15 μm) is only elongated to its full length when the gap is larger than twice the contour length (i.e., for 30 and 40 μm gaps), but is restricted to half the gap size otherwise (i.e., for 20 μm gaps). The same is true for the 48 kb DNA (20 μm), which only reaches its full length in 40 μm gaps.

IV. CONCLUSIONS

When exposed to a high frequency ac electric field, DNA molecules stretch from a compact coil into an elongated conformation as a result of the forces exerted on them. By immobilizing the DNA molecules onto the electrodes, the contribution of the torque to the elongation of the DNA could be studied. The width of the fluorescent band of elongated DNA around the electrodes was used to quantify the elongation and orientation.

We investigated the elongation and orientation of surface-bound DNA molecules of different sizes as a function of electric field magnitude and frequency. Maximum elongation was found for all different-sized fragments around 200–300 kHz. We found that elongation was only possible in fields higher than 0.06 MV/m. Above an applied voltage of 20 V, owing to the electrothermal fluid flow, no stable fluorescent band could be formed.

Our findings are compatible with an elongation mechanism based on the alignment of the DNA molecule segments with the electric field lines by the torque acting on the induced dipole in the molecule in conjunction with a bias force. We studied the electrohydrodynamic fluid flow by investigating the movement of fluorescently labeled latex beads during application of ac electric fields and we found that fluid flow occurred over the whole frequency range investigated, even at low electric field magnitudes. The fluid flow was always outwards from the electrode edges, and its velocity increased with decreasing frequency. This fluid flow results in a viscous drag force acting on the DNA during dielectrophoresis, thus supplying the torque with a directional bias pointing away from the electrode edge.

At low frequencies ($<$100 kHz) the elongation decreased with decreasing frequency and was below the detection limit at 45 kHz, even though the fluid flow was larger than at 300 kHz. This decay is due to a decrease of the torque owing to electrode polarization. At high frequencies ($>$400 kHz), the elongation decreased with increasing frequency as a result of the decreasing torque and decreasing fluid flow and thus bias force, leading to smaller elongation of the DNA. We conclude that the torque, complemented by a directional bias force, provides the major contribution to the elongation of the DNA.

By normalizing the elongation of the various DNA fragments with respect to their contour lengths as a function of electric field magnitude, we found that the contour length of the DNA has little influence on the normalized elongation of the DNA at a particular electric field frequency and magnitude, suggesting that the force acting on each segment of the DNA is uniform over most of the molecule.

Further, we investigated the influence of the electrode separation on the elongation of DNA. We found that DNA with contour lengths shorter than half the width of the gap elongated fully, while larger molecules were limited to half the distance between the electrodes. A maximum length of about 10 μm was observed for all the DNA molecules, except the 15 kb (6.5 μm) molecule, using an electric field of 1 MV/m to stretch the DNA across a 20 μm gap. These results, where the dielectrophoresis experiments were conducted on electrodes with various separations, further support the proposed elongation mechanism.

ACKNOWLEDGMENTS

This research was in part funded by the EPSRC. The authors would like to thank A. E. Cohen for helpful discussions. W.A.G. acknowledges the Cambridge Commonwealth Trust, C.W. acknowledges the Schweizerische Nationalfonds zur Förderung der wissenschaftlichen Forschung, and R.W. thanks the Gottlieb Daimler and Karl Benz-Stiftung for financial support. A.G.D. acknowledges the Royal Society.

[1] H. A. Pohl, *Dielectrophoresis* (Cambridge University Press, Cambridge, 1978).
[2] J. Gimsa, Bioelectrochem. Bioenerg. **54**, 23 (2001).
[3] M. P. Hughes, Nanotechnology **11**, 124 (2000).
[4] T. B. Jones, *Electromechanics of Particles* (Cambridge University Press, Cambridge, 1995).
[5] N. G. Green, A. Ramos, and H. Morgan, J. Phys. D **33**, 632 (2000).
[6] A. Ramos *et al.*, J. Phys. D **31**, 2338 (1998).
[7] A. D. Mehta *et al.*, Science **283**, 1689 (1999).
[8] M. D. Wang, Curr. Opin. Biotechnol. **10**, 81 (1999).
[9] W. Bowen, R. W. Lovitt, and C. Wright, Biotechnol. Lett. **22**, 893 (2000).
[10] H. G. Hansma, Annu. Rev. Phys. Chem. **52**, 71 (2001).
[11] J. Suehiro and R. Pethig, J. Phys. D **31**, 3298 (1998).
[12] Y. Huang *et al.*, Anal. Chem. **73**, 1549 (2001).
[13] G. H. Markx, P. A. Dyda, and R. Pethig, J. Biotechnol. **51**, 175 (1996).
[14] H. Morgan and N. G. Green, J. Electrost. **42**, 279 (1997).
[15] N. G. Green and H. Morgan, J. Phys. D **30**, 41 (1997).
[16] T. Muller *et al.*, J. Phys. D **29**, 340 (1996).
[17] C. L. Asbury, A. H. Diercks, and G. Van der Engh, Electrophoresis **23**, 2658 (2002).
[18] F. Dewarrat, M. Calame, and C. Schonenberger, Single Mol. **3**, 189 (2002).
[19] M. Washizu *et al.*, IEEE Trans. Ind. Appl. **30**, 835 (1994).
[20] H. Kabata, W. Okada, and M. Washizu, Jpn. J. Appl. Phys., Part 1 **39**, 7165 (2000).
[21] M. Washizu *et al.*, IEEE Trans. Ind. Appl. **31**, 447 (1995).
[22] T. Yamamoto *et al.*, IEEE Trans. Ind. Appl. **36**, 1010 (2000).
[23] S. Suzuki *et al.*, IEEE Trans. Ind. Appl. **34**, 75 (1998).
[24] W. A. Germishuizen *et al.*, Nanotechnology **14**, 896 (2003).
[25] R. Wirtz *et al.*, Nanotechnology **14**, 7 (2003).
[26] N. G. Green and H. Morgan, J. Phys. D **30**, 2626 (1997).
[27] N. G. Green *et al.*, Inst. Phys. Conf. Ser. **163**, 89 (1999).
[28] B. Ladoux and P. S. Doyle, Europhys. Lett. **52**, 511 (2000).
[29] M. L. Bennink *et al.*, Cytometry **36**, 200 (1999).
[30] J. F. Marko and E. D. Siggia, Macromolecules **28**, 8759 (1995).
[31] T. R. Strick *et al.*, Rep. Prog. Phys. **66**, 1 (2003).
[32] A. E. Cohen, Phys. Rev. Lett. **91**, 235506 (2003).
[33] H. Morgan and N. G. Green, *AC Electrokinetics: Colloids and Nanoparticles* (Research Studies, Baldock, UK, 2003).
[34] T. T. Perkins *et al.*, Science **268**, 83 (1995).
[35] R. Zimmermann and E. Cox, Nucleic Acids Res. **22**, 492 (1994).
[36] R. Paul and K. Kaler, J. Colloid Interface Sci. **194**, 225 (1997).
[37] S. Bone and C. A. Small, Biochim. Biophys. Acta **1260**, 85 (1995).
[38] B. Saif *et al.*, Biopolymers **31**, 1171 (1991).